Ancilla-Assisted Calibration of a Measuring Apparatus

G. Brida,[1] L. Ciavarella,[1] I. P. Degiovanni,[1] M. Genovese,[1] A. Migdall,[2] M. G. Mingolla,[1,3] M. G. A. Paris,[4,5,1] F. Piacentini,[1] and S. V. Polyakov[2]

[1]*Istituto Nazionale di Ricerca Metrologica, Strada delle Cacce 91, Torino 10135, Italy*
[2]*Joint Quantum Institute and National Institute of Standards and Technology, 100 Bureau Drive, Stop 8410, Gaithersburg, Maryland 20899, USA*
[3]*Dipartimento di Fisica, Politecnico di Torino, Corso Duca degli Abruzzi 24, Torino 10129, Italy*
[4]*Dipartimento di Fisica, Università degli Studi di Milano, Milano I-20133, Italy*
[5]*Consorzio Nazionale Interuniversitario per le Scienze Fisiche della Materia, Udr Milano, Milano I-20133, Italy*

(Received 23 March 2012; published 19 June 2012)

A quantum measurement can be described by a set of matrices, one for each possible outcome, which represents the positive operator-valued measure (POVM) of the sensor. Efficient protocols of POVM extraction for arbitrary sensors are required. We present the first experimental POVM reconstruction that takes explicit advantage of a quantum resource, i.e., nonclassical correlations with an ancillary state. A POVM of a photon-number-resolving detector is reconstructed by using strong quantum correlations of twin beams generated by parametric down-conversion. Our reconstruction method is more statistically robust than POVM reconstruction methods that use classical input states.

DOI: 10.1103/PhysRevLett.108.253601 PACS numbers: 42.50.Dv, 03.65.Ta, 42.50.Ar, 85.60.Gz

Measurements are at the heart of the scientific method because they allow us to gauge observables in experimental tests, leading either to the confirmation or to the ruling out of the scientific hypothesis. In quantum mechanics, measurements play a critical role because they connect the abstract description of quantum phenomena in Hilbert space to observable events. In the process of measurement, a quantum mechanical object interacts with a measurement device, and a measurement outcome is a result of such interactions. A complete quantum mechanical description of a measurement device is its positive operator-valued measure (POVM). In the quantum realm, sensor calibration corresponds to determining its POVM. In the last decade, the rapid development of innovative quantum technologies promoted POVMs from being an abstract theoretical tool to the experimental realm. In particular, precise and fully quantum characterization techniques for sensors [1–4] play a critical role for the implementation of quantum information processing, metrology, and imaging [5–16], as well as tomography of states [17–24] and operations [25–30]. Thus, quantum sensor characterization can be seen as a simultaneous measurement of multiple parameters; therefore, the efficiency of such a measurement is of utmost importance. However, POVM extraction has been experimentally pursued by brute force methods so far, i.e., by probing sensors with a suitably large set of interrelated input signals and classical states, yielding slow convergence [2,3]. It was shown [1] that taking advantage of quantum resources, e.g., entanglement, can improve convergence beyond the traditional methods. Here, we present the first experimental POVM reconstruction that explicitly uses a quantum resource, i.e., nonclassical correlations with an ancillary state [31]. Our experiment represents a major step forward towards quantum mechanical treatment of sensors: it demonstrates the reconstruction of an inherently quantum measure of an arbitrary detector's performance—its POVM—by realizing for the first time the method of Ref. [1].

A POVM is defined as a set of operators (matrices) Π_n that give the probability of the measurement outcomes via the Born rule $p_n = \mathrm{Tr}[\varrho\Pi_n]$, where ϱ is the density operator describing the system being measured. In principle, it is possible to extract a POVM of a photon detector using classical states of light (e.g., coherent states [2]) by inverting the Born rule after collecting data for a sufficiently large set of states. A direct inversion, however, is a rather delicate and mathematically unstable procedure, so that even a small uncertainty due to a finite statistical sample size can result in a large uncertainty in POVM matrix elements. Having a quantum source producing on-demand Fock states with a defined photon number would simplify the problem significantly, improving accuracy in the same measurement time by at least a factor of $\sqrt{N}$, where N is the number of possible measurement outcomes for a detector. Unfortunately, there are no ideal sources of photon number states. A measurement scheme based on nonclassically correlated bipartite systems (beyond $N = 1$) is an attractive alternative that realizes the full potential of the original scheme of [32]. In this case [1], one beam is sent to the detector under test (DUT) and the other (an ancilla state) to an ideal photon-number-resolving (PNR) detector (i.e., 100% efficiency and full photon number resolution), playing the role of what in the following we will address as a quantum tomographer. In this case, by using twin beams, one produces heralded (but not predefined) Fock states, thus yielding a measurement speedup of at least $\sqrt{N}$.

This alternative retains the statistical reliability advantage of the on-demand Fock state source. Even with an imperfect tomographer (i.e., efficiency <1 and no photon-number resolution), significant advantage over classical measurements can be retained. Thus, ancilla-assisted quantum schemes, where nonclassical correlations play a key role in improving both precision and stability, represent a practical advantage of quantum-enabled measurements over their classical counterparts.

Here we provide the first experimental implementation of this novel paradigm and demonstrate an effective reconstruction method for the POVM of an arbitrary detector, thus giving the full quantum characterization of its performance.

Let us assume that a bipartite system may be prepared in a given state described by the density operator ϱ_R, and that besides the measurement made by the detector to be calibrated, a known observable with a discrete set of outcomes is measured at the tomographer. In our scheme, the DUT is a phase-insensitive PNR detector, which represents one of the most critical components in quantum technology. The detector's POVM elements are diagonal operators in the Fock basis and may be written as $\Pi_n = \sum_m \Pi_{nm} |m\rangle\langle m|$, where Π_{nm} represents the probability of observing n counts when m photons are incident on a PNR detector (with the obvious constraint that $\sum_n \Pi_{nm} = 1$). Π_{nm} is the matrix element to be reconstructed by our measurement.

In our experiment, the bipartite state consists of the optical twin beams $\varrho_R = |R\rangle\langle\langle R|$, $|R\rangle\rangle = \sum_m R_m |m\rangle|m\rangle$, where $|m\rangle$ is the state of one beam with m photons; the tomographer is a simple yes or no detector with a selectable efficiency η defined as including all optical losses and assumes that the detector is live and ready to sense incoming light; and R_m is the probability amplitude of a particular $|m\rangle$ state. An experimental event is a detection of n photons at the DUT paired with a measurement outcome ("yes" or "no") at the tomographer, which occur with probabilities

$$p(n, \text{yes}) = \sum_m \Pi_{nm} |R_m|^2 [1 - (1 - \eta)^m] \quad \text{and}$$
$$p(n, \text{no}) = \sum_m \Pi_{nm} |R_m|^2 (1 - \eta)^m, \tag{1}$$

respectively. Upon collecting data to determine $p(n, \text{yes})$ and $p(n, \text{no})$, one may invert these relations and recover the unknown matrix elements Π_{nm} [31]. The distribution $|R_m|^2$ of the bipartite states is determined from the photon number distribution of the beam addressed to the tomographer, which is identical to its twin that is sent to the DUT. In this case, the data are the unconditional tomographer click events, which occur with probability $p(\text{no}) = \sum_m |R_m|^2 (1 - \eta)^m$, and allow reliable reconstruction of $|R_m|^2$'s [22] after collecting data at different system detection efficiencies. Note that this procedure is much simpler than full quantum tomography [17–20], as no additional calibration is needed to determine the $|R_m|^2$ coefficients other than the calibration of the efficiencies at the tomographer. Notice also that entanglement is not needed to achieve this POVM reconstruction of a PNR detector. Instead, it is the strong nonclassical correlation that enhances the accuracy and stability of the reconstruction, thus highlighting the role of squeezing and ancilla states as a crucial technical resource for the development of photonic quantum technologies.

The experimental setup (Fig. 1) comprises an 800-nm mode-locked laser with a repetition rate of 76 MHz, doubled via second harmonic generation to 400 nm, which pumps a $LiIO_3$ crystal to produce degenerate, but noncollinear, photons using parametric down-conversion (PDC) with type I phase matching [5]. One of the beams from this crystal is sent to the tomographer that consists of a calcite polarizer (that allows changing the detection efficiency), an interference filter (with a passband of 20 nm, full width at half maximum), and a silicon single photon avalanche diode (SPAD). The beam is delivered to the SPAD through a multimode fiber, which defines the spatial collection of the light. Because the down-converted photons have the same linear polarization in both arms, the polarizer can be used to variably attenuate the input beam and hence change the efficiency of the tomographer. The other PDC beam is directed to our PNR DUT, a detector tree consisting of two Si-SPADs, through a coupling system similar to the tomographer path (i.e., an interference filter and a fiber coupler). This two-SPAD DUT is able to discriminate between three possibilities: 0, 1, and 2 or more photo detections per pulse. An event 0 is when neither SPAD clicks. An event 1 is when either SPAD clicks, but not both. An event 2 is when both SPADs click.

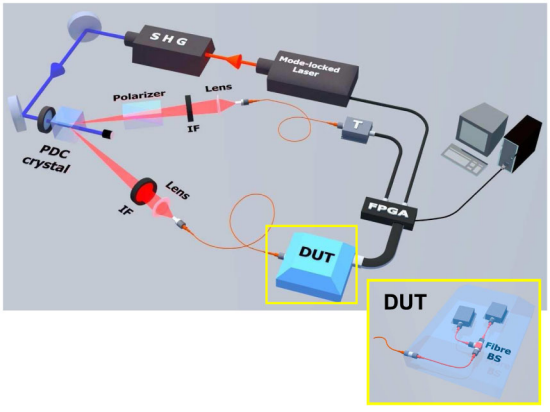

FIG. 1 (color online). Experimental setup: $LiLO_3$ crystal pumped with a pulsed 400-nm beam created through second harmonic generation (SHG) produces two correlated beams. One is sent to the tomographer (T), while its twin is sent to the DUT. The tomographer efficiency is varied by rotating the linear polarizer. Interference filters (IF) with 20-nm bandpasses are used to limit out-of-band light on the detectors. A FPGA is used for real-time processing and data acquisition. The DUT (inset) is a PNR detector made of two Si-SPADs connected through a 50:50 fiber beam splitter (BS).

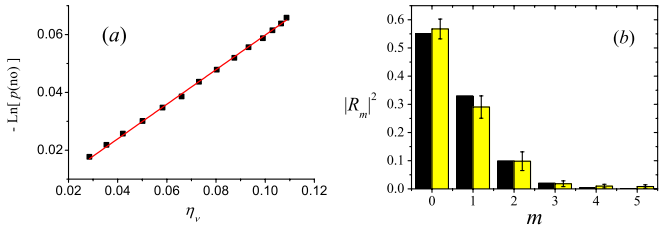

FIG. 2 (color online). (a) A linearized Poisson distribution with respect to detection efficiency. The best fit (line) of the $p(\text{no})$ data (points) yields a Poisson distribution with $\mu = 0.5983 \pm 0.0017$ mean photons per pulse. (b) The reconstructed bipartite state $|R_m|^2$ distribution (light colored bars), compared to a Poisson distribution (black bars) with the photon number determined by the fit in (a). Uncertainties shown represent the one σ variations in the reconstructions performed on 30 different data sets.

The outputs of the two Si-SPADs of our PNR detector, together with the tomographer output and a trigger pulse (from the laser), are sent to a field programmable gate array (FPGA) based processing and data collection system. We distinguish the three possible outcomes of the DUT along with the results of the tomographer measurements. Because detectors have dead time, the FPGA is programmed to avoid taking data when either of the detectors in the system is not ready. Before the data acquisition, the tomographer arm polarizer is calibrated to provide the 20 different system efficiencies that are needed for the experiment.

To reconstruct the POVM of our DUT, we first determine the relative frequencies $f(0)$, $f(1)$, and $f(2)$, respectively from the number of 0-, 1-, and 2-click events normalized to their sum. We also determine the relative frequencies of conditional events paired with the tomographer's clicks $[f(\text{yes}|0, \eta_\nu), f(\text{yes}|1, \eta_\nu), f(\text{yes}|2, \eta_\nu)]$, and no-clicks $[f(\text{no}|0, \eta_\nu), f(\text{no}|1, \eta_\nu), f(\text{no}|2, \eta_\nu)]$ for each efficiency η_ν. As mentioned above, the preliminary step in obtaining the POVM elements is the reconstruction of the photon number distribution $|R_m|^2$ [22] of the bipartite state. Figure 2(a) fits the $p(\text{no})$ data to a Poisson distribution with $\mu = 0.5983 \pm 0.0017$ mean photons per pulse. This is then used to reconstruct the bipartite state $|R_m|^2$ distribution seen in Fig. 2(b). The experimentally reconstructed photon distribution is in excellent agreement with the Poisson distribution, with a fidelity larger than 99.4% (here and in the following, we use the conventional definition of fidelity as the sum of the square root of the product of the experimental and the theoretical probabilities [22]). Data are shown only up to $m = 5$ photons since in our experiment the probability of observing more than five photon pairs per pulse is negligible (less than 4×10^{-4}). We then substitute the reconstructed $|R_m|^2$'s together with the set of calibrated efficiencies $\{\eta_\nu\}$ into Eq. (1), and reconstruct the quantities Π_{nm} using a regularized least-square method [2,3] to minimize the deviation between the measured and theoretical values of the probabilities. In particular, for each output n of the DUT, we minimize the deviation between the observed $p_{\text{exp}}(n, \text{yes}) = f(n)f(\text{yes}|n, \eta_\nu)$ and the theoretical probabilities $p(n, \text{yes})$ if an event n coincided with a click on a tomographer, and between $p_{\text{exp}}(n, \text{no}) = f(n)f(\text{no}|n, \eta_\nu)$ and $p(n, \text{no})$ if an event n was not correlated to a click of a tomographer. This is done for each η_ν.

The reconstructed Π_{0m}, Π_{1m}, and Π_{2m} are presented in Fig. 3 for input states with up to $m = 5$ photons. For the first five values (i.e., $m \leq 4$), the high fidelities (larger than 99.9%) and low uncertainties highlight the excellent agreement between the theoretical and experimental results. The quality of the POVM reconstruction rapidly decreases for $m > 4$ because of the lack of high photon number events, as discussed in connection with Fig. 2. Note that this limitation is not inherent to our calibration method. In practice, estimating the probabilities with sufficient accuracy in the photon number range of interest in a finite measurement time requires a bipartite state with enough Fock states in that range; our twin beam source produces enough states up to $m = 4$.

To assess the reliability of the reconstruction, we compare the measured probabilities $p_{\text{exp}}(n, \text{on})$ and

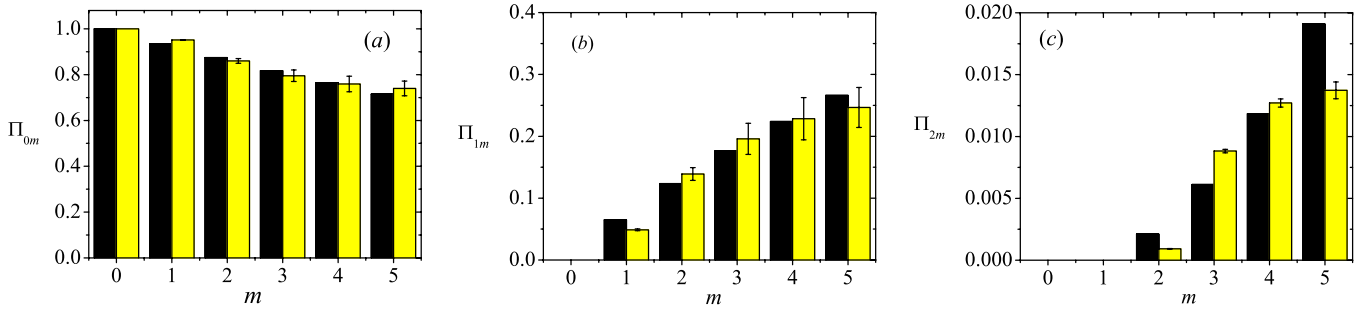

FIG. 3 (color online). Reconstruction of the POVM elements for photon numbers up to $m = 5$. Experimentally reconstructed (light-colored bars) and theoretical (black bars) histograms for (a) Π_{0m}, (b) Π_{1m}, and (c) Π_{2m}. The quality of the reconstruction of POVM elements with $m < 5$ is independently confirmed by observed fidelities above 99.9%. As expected, the accuracy starts deteriorating for input states with $m \geq 5$. The uncertainty bars represent the statistical fluctuations in the reconstructions performed on 30 different data sets.

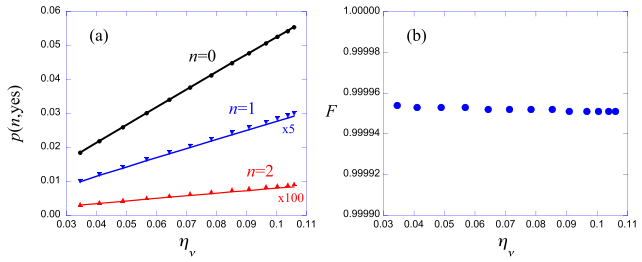

FIG. 4 (color online). (a) Comparison between measured (points) and theoretical (lines) probabilities, $p(n, \text{yes})$, for $n = 1$, 2, and 3, for each measurement η_ν. Probabilities for $n = 2$ and 3 are scaled by 5 and 100, respectively. Theoretical probabilities are obtained by substituting the measured values of the efficiencies η_ν, the reconstructed POVM, and the reconstructed $|R_m|^2$ into Eq. (1). Panel (b) demonstrates the agreement between the theory and experimental data in terms of fidelity.

$p_{\text{exp}}(n, \text{off})$ with the ones obtained from Eq. (1) using the reconstructed POVM and the reconstructed state (see Fig. 4). The excellent agreement, as seen by the near-unity fidelities, confirms that the reconstructed POVM provides a reliable quantum description of the detection process.

In conclusion, we have experimentally reconstructed the POVM of a photon-number-resolving detector by exploiting the quantum correlation of a twin-beam state. The reconstructed POVM elements are in excellent agreement with the theoretically expected ones, as witnessed by their fidelities, always above 99.9% for up to four incoming photons. Our results represent a major step towards quantum photonics for two reasons. First, this is the first experimental demonstration of an enhanced ancilla-assisted quantum detector tomography. We demonstrated the reconstruction of an inherently quantum measure of an arbitrary detector's performances—its POVM. Second, in view of the development of novel PNR detectors with improved efficiency, timing jitter, and dynamic range, we expect a dramatic growth in the demand of robust, reliable, and fully quantum characterization methods, with emphasis on those exploiting quantum resources to go beyond the limits of classical measurement.

The research leading to these results has received funding from the European Union on the basis of Decision No. 912/2009/EC (project IND06-MIQC) from the MIUR, FIRB Grants No. RBFR10YQ3H and No. RBFR10UAUV, and by Compagnia di San Paolo. We thank Valentina Schettini and Mario Dagrada for collaborating in the early stage of preparing the setup.

[1] G. M. D'Ariano, L. Maccone, and P. Lo Presti, Phys. Rev. Lett. **93**, 250407 (2004).
[2] J. S. Lundeen, A. Feito, H. Coldenstrodt-Ronge, K. L. Pregnell, Ch. Silberhorn, T. C. Ralph, J. Eisert, M. B. Plenio, and I. A. Walmsley, Nature Phys. **5**, 27 (2009).
[3] G. Brida, L. Ciavarella, I. P. Degiovanni, M. Genovese, L. Lolli, M. G. Mingolla, F. Piacentini, M. Rajteri, E. Taralli, and M. G. A. Paris, arXiv:1103.2991 [New J. Phys. (to be published)].
[4] D. Mogilevtsev, Phys. Rev. A **82**, 021807(R) (2010).
[5] M. Genovese, Phys. Rep. **413**, 319 (2005) and references therein.
[6] I. Marcikic, H. de Riedmatten, W. Tittel, H. Zbinden, M. Legré, and N. Gisin, Phys. Rev. Lett. **93**, 180502 (2004).
[7] D. Bouwmeester, J.-W. Pan, K. Mattle, M. Eibl, H. Weinfurter, and A. Zeilinger, Nature (London) **390**, 575 (1997).
[8] D. Boschi, S. Branca, F. DeMartini, L. Hardy, and S. Propescu, Phys. Rev. Lett. **80**, 1121 (1998).
[9] J. L. O'Brien, Science **318**, 1567 (2007); P. J. Shadbolt, M. R. Verde, A. Peruzzo, A. Politi, A. Laing, M. Lobino, J. C. F. Matthews, M. G. Thompson, and J. L. O'Brien, Nature Photon. **6**, 45 (2012).
[10] P. G. Kwiat, S. Barraza-Lopez, A. Stefanov, and N. Gisin, Nature (London) **409**, 1014 (2001).
[11] T. Yamamoto, M. Koashi, S. K. Ozdemir, and N. Imoto, Nature (London) **421**, 343 (2003).
[12] J. W. Pan, C. Simon, and A. Zellinger, Nature (London) **410**, 1067 (2001).
[13] C. Sayrin *et al.*, Nature (London) **477**, 73 (2011).
[14] V. Boyer, A. M. Marino, R. C. Pooser, and P. D. Lett, Science **321**, 544 (2008).
[15] G. Brida, M. Genovese, and I. Ruo Berchera, Nature Photon. **4**, 227 (2010).
[16] V. Giovannetti, S. Lloyd, and L. Maccone, Phys. Rev. Lett. **96**, 010401 (2006).
[17] K. Vogel and H. Risken, Phys. Rev. A **40**, 2847 (1989).
[18] G. M. D'Ariano, C. Macchiavello, and M. G. A. Paris, Phys. Rev. A **50**, 4298 (1994).
[19] U. Leonhardt, M. Munroe, T. Kiss, Th. Richter, and M. G. Raymer, Opt. Commun. **127**, 144 (1996); M. Asorey, P. Facchi, G. Florio, V. I. Manko, G. Marmo, S. Pascazio, and E. C. G. Sudarshan, Phys. Lett. A **375**, 861 (2011); Y. Bogdanov, G. Brida, M. Genovese, S. P. Kulik, E. V. Moreva, and A. P. Shurupov, Phys. Rev. Lett. **105**, 010404 (2010); M. Vasilyev, S. K. Choi, P. Kumar, and G. M. D'Ariano, Phys. Rev. Lett. **84**, 2354 (2000).
[20] G. Breitenbach, S. Schiller, and J. Mlynek, Nature (London) **387**, 471 (1997).
[21] A. Agliati, M. Bondani, A. Andreoni, G. De Cillis, and M. G. A. Paris, J. Opt. B **7**, S652 (2005).
[22] G. Zambra, A. Andreoni, M. Bondani, M. Gramegna, M. Genovese, G. Brida, A. R. Rossi and M. G. A. Paris, Phys. Rev. Lett. **95**, 063602 (2005).
[23] A. Allevi, A. Andreoni, M. Bondani, G. Brida, M. Genovese, M. Gramegna, P. Traina, S. Olivares, M. G. A. Paris, and G. Zambra, Phys. Rev. A **80**, 022114 (2009).
[24] J. Rehacek, D. Mogilevtsev, and Z. Hradil, Phys. Rev. Lett. **105**, 010402 (2010); Z. Hradil, D. Mogilevtsev, and J. Rehacek, Phys. Rev. Lett. **96**, 230401 (2006).
[25] G. M. D'Ariano and P. Lo Presti, Phys. Rev. Lett. **86**, 4195 (2001).
[26] J. B. Altepeter, D. Branning, E. Jeffrey, T. C. Wei, P. G. Kwiat, R. T. Thew, J. L. O'Brien, M. A. Nielsen, and A. G. White, Phys. Rev. Lett. **90**, 193601 (2003).
[27] J. L. O'Brien, G. J. Pryde, A. Gilchrist, D. F. V. James, N. K. Langford, T. C. Ralph, and A. G. White, Phys. Rev. Lett. **93**, 080502 (2004).

[28] M. Lobino, D. Korystov, C. Kupchak, E. Figueroa, B. C. Sanders, and A. I. Lvovsky, Science **322**, 563 (2008).

[29] I. Bongioanni, L. Sansoni, F. Sciarrino, G. Vallone, and P. Mataloni, Phys. Rev. A **82**, 042307 (2010).

[30] S. Rahimi-Keshari, A. Scherer, A. Mann, A. T. Rezakhani, A. I. Lvovsky, and B. C. Sanders, New J. Phys. **13**, 013006 (2011).

[31] This is in contrast to ancilla-based detector calibrations, [for an example, see A. P. Worsley *et al.*, Opt. Express **17**, 4397 (2009)], which require assumptions (i.e., detector linearity) and are aimed at extracting a single detection efficiency parameter rather than the more extensive quantum description (POVM).

[32] B. Ya. Zeldovich and D. N. Klyshko, JETP Lett. **9**, 40 (1969).